F-aza-T-dCyd (NSC801845), a novel cytidine analog, in comparative cell culture and xenograft studies with the clinical candidates T-dCyd, F-T-dCyd and aza-T-dCyd

Joel Morris[1,4], **Donn G. Wishka**[1], **Omar D. Lopez**[1], **Vladimir Rudchenko**[2], **Guangfei Huang**[2], **Sierra N. Hoffman**[3], **Suzanne Borgel**[3], **Kyle Georgius**[3], **John Carter**[3], **Howard Stotler**[3], **Mark W. Kunkel**[1], **Jerry M. Collins**[1], **Melinda G. Hollingshead**[1], **Beverly A. Teicher**[1]

[1]Developmental Therapeutics Program, Division of Cancer Treatment and Diagnosis, The National Cancer Institute, Rockville, MD, 20852

[2]Alchem Laboratories Corporation, Alachua, FL 32615

[3]Leidos Biomedical Laboratories, FNLCR, Frederick, MD 21702

Abstract

Herein 5-Aza-4'-thio-2'-β-fluoro-2'-deoxycytidine (F-aza-T-dCyd, NSC801845), a novel cytidine analog, is first disclosed and compared with T-dCyd, F-T-dCyd and aza-T-dCyd in cell culture and mouse xenograft studies in HCT-116 human colon carcinoma, OVCAR3 human ovarian carcinoma, NCI-H23 human NSCLC carcinoma, HL-60 human leukemia, and the PDX BL0382 bladder carcinoma. In three of five xenograft lines (HCT-116, HL-60 and BL-0382), F-aza-T-dCyd was more efficacious than aza-T-dCyd. Comparable activity was observed for these two agents against the NCI-H23 and OVCAR3 xenografts. In the HCT-116 study, F-aza-T-dCyd (10 mg/kg IP, QDx5 for 4 cycles), produced complete regression of the tumors in all mice with a response that proved durable beyond post-implant day 150 (129 days post-last dose). Similarly, complete tumor regression was observed in the HL-60 leukemia xenograft when mice were dosed with F-aza-T-dCyd (10 mg/kg IP, QDx5 for 3 cycles). In the PDX BL-0382 bladder study, both oral and IP dosing of F-aza-T-dCyd (8 mg/kg QDx5 for 3 cycles) produced regressions that showed tumor regrowth beginning 13-days post dosing. These findings indicate that further development of F-aza-T-dCyd (NSC801845) is warranted.

Keywords

cytidine analogs; NCI60 screen

INTRODUCTION

Cytidine analogs remain an area of active drug discovery and development with five FDA approved drugs, including cytarabine which was approved in 1969 for the treatment of acute myeloid leukemia (AML) (1). DNMT1, a maintenance methyltransferase that contributes to

[4]**Corresponding author**: Joel Morris, PhD, Chief, Drug Synthesis and Chemistry Branch, National Cancer Institute, 9609 Medical Center Drive, Bethesda, MD 20892, Phone: 240-276-5953, FAX: 240-276-7895, joel.morris@nih.gov, morrisj5@mail.nih.gov.

the hypermethylation and silencing of tumor suppressor genes, is a major molecular target of two of these drugs, azacytidine and decitabine which were approved for myelodysplastic syndromes in 2004 and 2006, respectively (2). The latter two drugs have also been tested in leukemia and solid tumor clinical trials as single agents and in combination therapies (3). When DNMT1 is depleted by drug treatment, the existing methyl pattern on genes is no longer maintained in replicated cells resulting in reactivation of tumor suppressor genes (4). At least two cell division cycles are required after drug exposure to maximize re-expression of silenced genes (2). In addition, DNMT1 has roles independent of its methyltransferase activity and a DNMT1 knockout results in decreased cell viability preceded by events consistent with activation of a DNA damage response. Azacytidine and decitabine contain aza-cytosine bases connected to a ribose ring that is notable by the presence or absence of a hydroxy group at the 2-position. 4'-thio-2'-deoxycytidine (T-dCyd) and 5-aza-4'-thio-2'-deoxycytidine (aza-T-dCyd) are two related sulfur-containing deoxy-cytidine analogs that deplete DNMT1 both *in vitro* and *in vivo* in tumor cells (5). Both agents were effective (IP dosing) in slowing the growth of tumors in NCI-H23 human NSCLC xenografts in athymic nude mice (nu/nu NCr). T-dCyd and aza-T-dCyd are currently in Phase I clinical trials at The National Cancer Institute (NCT02423057 and NCT03366116, respectively). The representative examples of cytidine agents are shown in Figure 1.

The incorporation of a fluorine atom into the chemical structure of cytidine derivatives has been an effective strategy for modulating the pharmacokinetic and pharmacodynamic parameters of the nucleoside (6). Through the ability of fluorine to increase lipophilicity and affect electronic and steric factors, fluorine atoms can be used to block metabolism and produce changes in target potency, selectivity, and overall toxicity associated with the modified derivative. Gemcitabine is a widely clinically used fluorine containing cytidine drug that is approved for use in pancreatic, ovarian, breast and non-small cell lung cancers. Gemcitabine is a prodrug which is phosphorylated intracellularly and incorporated into DNA during DNA synthesis, thus, terminating further DNA chain elongation (7–9). DNA repair processes are unable to remove gemcitabine resulting in cell death. RX-3117 is another fluorine containing agent that can downregulate DNMT-1 and can be incorporated into RNA and DNA (10). RX-3117 has shown significant efficacy in several colon, lung, and pancreatic human xenograft models including against tumor lines that are resistant to gemcitabine (11). RX-3117 has completed Phase 1 trial and has undergone Phase 2 trial in metastatic bladder cancer as a single agent and Phase 2 trial in metastatic pancreatic cancer in combination with abraxane (NCT02030067 and NCT03189914). FF-10502 (F-T-dCyd) is a fluorine-containing thio-nucleoside that inhibits DNA-polymerase and is superior to gemcitabine in targeting pancreatic cancer cells (12). FF-10502 is currently in Phase 1/2 clinical trial in solid tumors and lymphomas (13). (NCT02661542).

Herein the synthesis and first disclosure of a novel fluorine containing cytidine analog, 5-aza-4'-thio-2'-β-fluoro-2'-deoxycytidine (F-aza-T-dCyd, NSC801845), is described (14). F-aza-T-dCyd is compared to several related cytidine analogs (including T-dCyd, aza-T-dCyd and F-T-dCyd (FF-10502)), in the NCI-60 cell assay. In addition, the results of a comparative *in vivo* efficacy study are presented with F-aza-T-dCyd, gemcitabine, T-dCyd, aza-T-dCyd, and FF-10502 in several human tumor xenograft studies, including HCT-116 human colon carcinoma, OVCAR3 human ovarian carcinoma, NCI-H23 human NSCLC

carcinoma, and HL-60 human leukemia as well as a patient-derived xenograft, BL0382 bladder carcinoma.

MATERIALS AND METHODS

Compound Synthesis.

The FDA-approved drugs, 5-azacytidine, decitabine and gemcitabine, were obtained from the DTP chemical repository (available from NCI at: https://dtp.cancer.gov/organization/dscb/obtaining/default.htm). The investigational agent RX-3117 was purchased from ChemScene. T-dCyd and aza-TdCyd were synthesized as described (15). FF-10502 (F-T-dCyd) was synthesized at NCI according to a modification (14) of methods described (16). Briefly, NSC-801845 was synthesized in 13 steps as described in Figure 2 (14). A detailed description and experimental details for the syntheses of F-aza-T-dCyd (NSC-801845) and FF-10502 are found in the supplemental material.

Cell Culture.

NCI-60 cell lines were obtained from the NCI Developmental Therapeutics Program Tumor Repository. For each lot of cells, the Repository performed Applied Biosystems AmpFLSTR Identifiler testing with PCR amplification to confirm consistency with the published Identifiler STR profile for the given cell line (17–19). Each cell line was tested for mycoplasma when it was accepted into the repository; routine mycoplasma testing of lots was not performed. Cells were kept in continuous culture for no more than 20 passages. The optimal seeding densities for each of the cell lines at each time point assessed were determined prior to performing the concentration response studies (20–22). The NCI-60 screen was performed as described at: https://dtp.cancer.gov/discovery_development/nci-60/default.htm. Briefly, the NCI-60 human tumor lines were grown in RPMI 1640 medium supplemented with 5% FBS and 2 mM L-glutamine. For experiments, cells were inoculated into 96-well plates in 100 μL of complete medium at plating densities ranging from 5,000 to 40,000 cells/well depending on the doubling time of individual lines. The plates were incubated at 37° C in humidified 5 % CO_2/95 % air for 24 h. Compounds were formulated in DMSO. The plates were incubated for 48 h. For staining, sulforhodamine B (SRB) solution (100 μl) at 0.4 % (w/v) in 1 % acetic acid was added to each well, and plates were incubated for 10 min at room temperature. The SRB was solubilized, and the absorbance at 515 nm was read. Using the absorbance measurements [time zero, (Tz), control growth, (C), and test growth (Ti), the percent cell growth was calculated. Growth inhibition of 50 % (GI50) is calculated from $[(Ti-Tz)/(C-Tz)] \times 100 = 50$, which is the compound concentration resulting in a 50% reduction in the net protein increase (as measured by SRB staining) in control cells.

In Vivo Studies.

Human tumor xenografts were generated in 4- to 6-week-old female athymic nude mice (nu/nu NCr) or NSG mice by subcutaneous injection of tumor cells (HL-60, NCI-H23, OVCAR-3, HCT-116) grown in vitro using RPMI 1640 with 10% fetal bovine serum and 2 mM l-glutamine (23).

The BL0382F1232 patient-derived xenograft (PDX) model, was originally developed by Jackson Laboratories and received from JAX as cryopreserved fragments (available as JAX # TM00020) (24). Upon receipt we serially passaged the tumor to create a cryopreserved bank of tumor fragments. For drugs studies, vials of cryopreserved tumor were thawed, implanted into NSG mice and the resulting tumors passaged into cohorts of mice to establish the study mice as described for other xenograft models (23).

The mice were housed in an AAALAC accredited facility with food and water provided ad libitum. When tumors reached the predetermined starting weight (staging weight), the animals were randomized into experimental groups and treatment was initiated. Groups included a vehicle control group as well as the drug-treated groups. Drug doses were selected based upon prior experience or newly conducted mouse tolerability studies as described elsewhere (23). Tumors were monitored by bidirectional caliper measurements and the tumor weights were calculated as tumor weight (mg) = (tumor length in mm×tumor width in mm2)/2. Data collection was performed using the StudyLog software program StudyDirector [Studylog Systems, Inc., South San Francisco, CA]. Data were calculated and plotted using Microsoft EXCEL. Significant differences in response between controls and each treatment group were calculated using student's t-test.

RESULTS

Synthesis of F-aza-T-dCyd (NSC801845)

The incorporation of a fluorine atom into the cytidine aza-T-dCyd was accomplished starting from the commercially available (2R,3S,4R,5R)-5-((benzoyloxy)methyl)-3-fluorotetrahydrofuran-2,4-diyl dibenzoate. Primarily utilizing chemistry applied previously to the synthesis of the des-fluoro-thio sugar, the intermediate 2-bromo-3-β-fluoro thio sugar was prepared in 11 steps and immediately coupled with silylated aza-cytosine to produce upon deprotection F-aza-T-dCyd (NSC801845) (14). A comparison of calculated LogP values (cLogP values obtained from ChemDraw v.18) for aza-T-dCyd (−4.37) and F-aza-T-dCyd (−3.93) suggests a lipophilicity increase of a half log value for the novel fluorinated agent (Figure 3).

Cell Culture Studies

The eight cytidine agents were evaluated in the 5-concentration NCI60 cell line assay (Figure 3). Representative concentration response curves from four of the NCI60 cell lines showed a 10-fold to 100-fold difference in sensitivity of the cells to the eight compounds (Figure 3). The most cytotoxic compounds were gemcitabine, FF-10502 (F-T-dCyd), F-aza-T-dCyd (NSC801845), followed by RX-3117. The least cytotoxic compounds were decitabine and T-dCyd. The NCI60 heatmap based upon the GI$_{50}$ values showed the full range of activity in the assay and indicated some similarities in the patterns of cell line sensitivities for some of the eight compounds. The hematological malignancy cell lines were generally sentive to the compounds except TdCyd. Among the NSCLC lines, NCI-H460 was sensitive while EKVX and NCI-H226 were less responsive. With the exception of gemcitabine and FF-10502 (F-T-dCyd), the CNS malignancy cell lines were generally non-responsive. MDA-MB-435 was most sensitive among the melanoma lines and SK-Mel-2 and

SK-Mel-5 were the least responsive. The ovarian cancer line OVCAR8 was sensitive to the cytidine analogs while the ovarian cancer cell line OVCAR-4 was generally non-responsive to the cytidine analogs. Among the renal cell carcinoma cell line panel, the ACHN cell line was very responsive and the TK-10 cell line was the least responsive. The breast and prostate cancer panel cell lines had mixed-responses to the eight cytidine analogs with only MCF-7 showing relative sensitivity to the group.

A GI_{50} matrix grid-COMPARE analysis, employing a standard Pearsons correlation, run with the eight cytidine analogs revealed a strong COMPARE correlation between F-aza-T-dCyd (NSC801845) and FF-10502 (F-T-dCyd) (0.89) as well as between gemcitabine and F-aza-T-dCyd (NSC-801845) (0.68) and between gemcitabine and FF-10502 (F-T-dCyd) (0.74) (Figure 3C). Examination of the corresponding mean graphs of F-aza-T-dCyd, F-T-dCyd and gemcitabine further demonstrates the similarities between the NCI-60 patterns between these agents (Figure S1). The carbocyclic sugar analog, RX-3117 also showed interesting COMPARE correlations with strong correlation with aza-T-dCyd (0.67) and F-aza-T-dCyd (NSC801845) (0.65) with somewhat lower correlations to FF-10502 (F-T-dCyd) (0.57) and gemcitabine (0.47). Interestingly, the correlation between F-aza-T-dCyd (NSC801845) and aza-T-dCyd was relatively low (0.45). TGI and LC50 values were not examined in a COMPARE analysis since neither parameter was reached at 100 uM for any of the cytidine agents except gemcitabine.

In vivo Studies

In vivo studies were carried out with 5 of the 8 cytidine agents ,T-dCyd, aza-T-dCyd, gemcitabine, FF-10502 (F-T-dCyd) and F-aza-T-dCyd (NSC801845) in mouse xenograft studies with 5 tumor types, including HCT-116 human colon carcinoma , OVCAR3 human ovarian carcinoma, NCI-H23 human NSCLC carcinoma, HL-60 human leukemia and the patient-derived xenograft BL0382 human bladder carcinoma. (Figures 4–6). Doses and schedules for the known cytidine agents (T-dCyd and aza-T-dCyd (5), gemcitabine (25), F-T-dCyd (12)) were chosen at or near the maximum tolerated dose (MTD) previously observed in these and other tumor-bearing models. For F-aza-T-dCyd, an MTD was determined for single and multiple daily IP dosing and these doses and schedules were used in the five xenograft studies which were carried out in a sequential and iterative fashion (26). For example, with the observation of noteworthy activity for F-aza-T-dCyd in the HL-60 and HCT-116 xenografts, an oral dosed arm for this agent was added to the OVCAR-3 and BL0382 studies. In xenograft studies, T-dCyd was the least effective of the cytidine analogs in four of five xenografts. In three of five xenograft lines (HCT-116, HL-60 and the PDX BL-0382), F-aza-T-dCyd (NSC801845) was more efficacious than aza-T-dCyd (administered at the MTD of 1.5 mg/kg, IP). Comparable activity was observed for these two agents against the NCI-H23 and OVCAR3 xenografts.

In the HCT-116 study, F-aza-T-dCyd (NSC801845) (10 mg/kg IP, QDx5 for 4 cycles), produced complete regression of the tumors in all mice with a response that proved durable out to 150 days (129 days post-last dose) ($p = 8 \times 10^{-9}$) (Figure 4). In the HCT-116 model, regression was also observed with FF-10502 (F-T-dCyd) (240 mg/kg, IV, Q7D for 4 cycles), however tumor regrowth was observed upon cessation of treatment ($p = 1 \times 10^{-8}$). Both aza-

T-dCyd and gemcitabine provided modest suppression of tumor growth as well in the HCT116 tumor (p =1 × 10^{-7} and p = 1 × 10^{-7}, repectively). A once weekly dose of F-aza-TdCyd (400 mg, IP, for 3 cycles) in this study was also effective in initially causing regression in the HCT116 tumor (p = 1 × 10^{-8}), but this treatment proved to be less durable over time compared with 5 daily doses for 4 cycles. Mean body weights in the HCT-116-bearing animals were decreased initially with F-aza-T-dCyd treatment but recovered to normal levels of growth throughout the remainder of the study. Similar body weight effects were observed with the dosing of other cytidine agents in this study.

A similar complete tumor regression was observed in the HL-60 leukemia xenografts when mice were dosed with F-aza-T-dCyd (10 mg/kg, IP, QDx5 for 3 cycles) with a response that proved durable out to 45 days (p = 3 × 10^{-8}) (Figure 4). Tumor regression was also observed with F-aza-T-dCyd (400 mg/kg, IP, Q7Dx3) (p =3 × 10^{-7}) or FF-10502 (240 mg/kg, IV, Q7Dx4) (p = 2 × 10^{-5}), but tumor growth in this model resumed after cessation of either treatment. The antitumor effects for treatment with aza-T-dCyd and gemcitabine were minimal and T-dCyd was ineffective in the HL-60 leukemia model. Mean body weights were generally unaffected by any of the cytidine treatment protocols in the HL-60 xenografts.

In the OVCAR3 ovarian tumor xenograft model, similar levels of tumor growth suppression were observed with F-aza-TdCyd (8 to 4 mg/kg, PO, QDx5), FF-10502 (200 mg/kg, IV, Q7Dx3), aza-T-dCyd (1.5 mg/kg, IP, QDx5), or gemcitabine (150 mg/kg, IP, Q7Dx3) (Figure 5). Treatment with F-aza-T-dCyd (250 mg/kg, IP) administered weekly was minimally effective in this model. Mouse body weights initially dropped slightly more than 10% upon initial treatment with F-aza-T-dCyd but recovered normally throughout the remainder of the xenograft study.

In the NCI H-23 NSCLC lung carcinoma xenograft model, none of the cytidine agents showed significant efficacy, with only F-T-dCyd (240 mg/kg, IV, Q7Dx3) and T-dCyd (1.5 mg/kg, IP, QDx5) having minimal effects on tumor growth suppression (Figure 5). No difference was observed between the effects of weekly and daily administered doses of F-aza-T-dCyd. Mouse body weights were generally unaffected by any of the cytidine treatment protocols in the NCI-H-23 NSCLC study.

In the PDX BL0382 bladder carcinoma, both oral and IP dosing of F-aza-T-dCyd (8 mg/kg PO, QDx5 for 3 cycles; 8 mg/kg QDx5 IP, QDx5 for 3 cycles) produced regressions that showed tumor regrowth 13-days post dosing though at a growth rate below that of the control group (Figure 6). Although drug levels in the blood were not determined, the similar efficacy observed at the same doses with the oral and IP routes of administration in this model suggests that F-aza-T-dCyd (NSC801845) has significant oral activity in mice. This level of efficacy compared quite well with that observed after treatment with gemcitabine (150 mg/kg, IP, Q7Dx3). A weekly dose of F-aza-T-dCyd (250 mg/kg, IP, Q7Dx3) proved somewhat less effective although there was good tumor growth control throughout the dosing period. Treatments with F-T-dCyd, aza-T-dCyd and T-dCyd were less effective in the BL-0382 patient-derived xenograft model. Mouse body weights were generally unaffected by any of the cytidine treatment protocols in this study.

DISCUSSION

The NCI-60 human tumor cell line panel, consisting of cell lines from nine tumor types, has been used to profile potential oncology chemotherapeutic agents for the past 25 years (20). In addition, the NCI-60 screen has proven to be a useful tool for the oncology research community to further its understanding of the biology of cancer and the molecular targets and mechanisms of action of new oncology agents. In this regard, the COMPARE algorithm has been a useful tool for the direct comparison of sensitivity patterns resulting from the effects of compounds on cell growth in the 2-day NCI-60 assay (27). The qualitative nature of these sensitivity patterns (irrespective of potency) can often be correlative to the target mechanisms associated with the test compounds (28). Independent of whether a specific molecular target has been identified, high COMPARE (Pearsons) correlation between two test compounds is often indicative of a shared molecular mechanism of action.

Of the eight cytidine agents evaluated in the NCI-60 cell line panel, FF-10502 (F-T-dCyd) and gemcitabine were generally more potent based on the their respective mean GI_{50} (growth inhibition) values across the entire panel. These two agents were followed by F-aza-T-dCyd (NSC801845), azacytidine, and RX-3117 with aza-T-dCyd and T-dCyd being less cytotoxic based on their respective mean GI_{50} potencies in the two-day assay. However, by COMPARE analysis, F-aza-T-dCyd (NSC801845) correlated highly with FF-10502 (F-T-dCyd) and gemcitabine (correlations 0.89 and 0.68, respectively), suggesting a possible shared DNA-damaging mechanism of action amongst these three agents. Interestingly, the GI_{50} sensitivity patterns between F-aza-T-dCyd and aza-T-dCyd have a low correlation (0.45), even though these two agents differ in structure by only the presence or absence of a single fluorine atom.

Although correlation of the sensitivity patterns from the NCI-60 screen can often be associated with mechanistic information, the link between potency in the cell-line assay and in vivo efficacy is not universally realized. In this set of compounds, the two most potent cell culture agents, FF-10502 (mean log GI_{50} −6.30) and gemcitabine (mean log GI_{50} −6.60), have readily detected antitumor activity in four of the five xenograft models. However, the overall impressive efficacy associated with F-aza-T-dCyd (NSC801845) which produced regression of tumors in three of five of the xenografts models is not predicted by its GI_{50} potencies (mean log GI_{50} −5.41) in the NCI-60 assay. Several parameters could be factors in accounting for the in vitro/in vivo disconnect surrounding F-aza-T-dCyd (NSC801845), including the nature of the 2-day cell assay, mechanism of action, pharmacokinetics of the agent in mice and compound residence time in cells. The data indicate the tumor regression is durable upon cessation of compound dosing and that oral delivery of F-aza-T-dCyd (NSC801845) produced efficacy on par with or greater than IP delivery, further highlights the attractive nature of this new cytidine agent. These xenograft data clearly demonstrate that F-aza-T-dCyd (NSC801845) has remarkable activity relative to the comparator set against multiple tumor lines. Thus, further characterization of this novel cytidine derivative as a potential anti-tumor agent is warranted.

Supplementary Material

Refer to Web version on PubMed Central for supplementary material.

Acknowledgement

REFERENCES

1. Jordheim LP, Durantel D, Zoulim F, Dumontet C. Advances in the development of nucleoside and nucleotide analogues for cancer and viral diseases. Nature Rev Drug Discov 2013; 12: 447–463. [PubMed: 23722347]

2. Stresemann C, Lyko F. Modes of action of the DNA methyltransferase inhibitors azacytidine and decitabine. Int J Cancer 2008; 123: 8–13. [PubMed: 18425818]

3. Tough DF, Tak PP, Tarakhovsky A, Prinjha RK. Epigenetic drug discovery: breaking through the immune barrier. Nature Rev Drug Discov 2016; 15: 835– 53. [PubMed: 27765940]

4. Dor Y, Cedar H. Principles of DNA methylation and their implications for biology and Medicine. Lancet 2018; 392: 777–86. [PubMed: 30100054]

5. Thottassery JV, Sambandam V, Allan PW, Maddry J, Maxuitenko YY, Tiwari K, Hollingshead M, Parker WB. Novel DNA methyltransferase-1 (DNMT1) depleting anticancer nucleosides, 4′-thio-2′-deoxycytidine and 5-aza-4′-thio-2′-deoxycytidine. Cancer Chemother Pharmacol 2014; 74: 291–302. [PubMed: 24908436]

6. Cavaliere A, Probst KC, Westwell AD, Slusarczyk M Fluorinated nucleosides as an important class of anticancer and antiviral agents. Future Med Chem 2017; 9(15):1809–1833. [PubMed: 28929804]

7. Plunkett W, Huang P, Gandhi V. Preclinical characteristics of gemcitabine. Anticancer Drugs 1995; 6 (suppl 6): 7–13.

8. Plunkett W, Huang P, Xu YZ, Heinemann V, Grunewald R, Gandhi V. Gemcitabine: metabolism, mechanisms of action and self-potentiation. Semin Oncol 1995; 22 (suppl 11): 3–10.

9. Muggia F, Diaz I, Peters GJ. Nucleoside and nucleobase analogs in cancer treatment: not only sapacitabine but also gemcitabine. Exp Opin Invest Drugs 2012; 21: 403–8.

10. Peters GJ, Smid K, Vecchi L, Kathmann I, Sarkisjan D, Honeywell RJ, Losekoot N, Ohne O, Orbach A, Blaugrund E, Jeong LS, Lee YB, Ahn CH, Kim DJ. Metabolism, mechanism of action and sensitivity profile of fluorocyclopentylcytosine (RX-3117; TV-1360). Invest New Drugs 2–13; 31: 1444–57.

11. Yang MY, Lee YB, Ahn C, Kaye J, Fine T, Kashi R, Ohne O, Smid K, Peters GJ, Kim DJ. A novel cytidine analog, RX-3117, shows potent efficacy in xenograft models, even in tumors that are resistant to gemcitabine. Cancer Res 2014; 34: 6951–6960.

12. Mima S, Kakinuma C, Higuchi T, Saeki K, Yamada T, Uematsu R, Ishino M, Kito N, Nishikawa H, Kuniyoshi H, Matsumoto T, Fujiwara H, Paradiso LJ, Shimada Y, Iwamura H. FF-10502, an antimetabolite with novel activity on dormant cells, is superior to gemcitabine for targeting pancreatic cancer cells. J Pharmacol Exp Ther 2018; 366:125–35. [PubMed: 29653962]

13. Janku F, Sen S, Pant S, Bramwell L, Subbiah V, Way T, et al. Phase 1/2 trial of FF-10502–01, a pyrimidine antimetabolite, in patients with advanced cholangiocarcinoma and solid tumors. J Clinical Oncol 2019; 37:suppl 3008.

14. Wishka DG, Morris J, Lopez OD 2'-Halogenated-4'-thio-2'-deoxy-5-azacytidine analogs and use thereof, WO 2020/068657.

15. (a)Morris J, Bahde R, Vishnuvajjala R, Wishka DG, Denysenko SM, Zhang L, Lopez OD. Stereoselective synthesis and process for the manufacturing of 2'-deoxynucleosides, WO 2019/152459.(b)Wishka DG, Lopez OD, Rudchenko VF, Huang G, Bahde R, Kumar V, Denysenko SM, Zhang L, Zhang M, Teicher BA, Morris J. The development of β-selective glycosylation reactions with benzyl substituted 2-deoxy-1,4-dithio-D-erythro-pentofuranosides: enabling practical multi- gram syntheses of 4'-Thio-2'-deoxycytidine (T-dCyd) and 5-aza-4'-thio-2'-deoxycytidine (aza- T-dCyd) to support clinical development. Nucleosides, Nucleotides & Nucleic Acids 2020; DOI: 10.1080/15257770.2020.1832694.

16. Nakamura K, Shimamura S, Imoto J, Takahashi M, Watanabe K, Wada K, Fujino Y, Matsumoto T, Takahashi M, Okada H, Yamane T, Ito T. Intermediate for synthesis of 1-(2-deoxy-2-fluoro-4-thio-b-D-arabinofuranosyl) cytosine, intermediate for synthesis of thionucleoside, and methods for producing these intermediates, WO 2014/027658

17. Plowman J; Dykes DJ Jr.; Hollingshead MG; Simpson-Herren L; Alley MC. Human tumor xenograft models in NCI drug development. In: Teicher BA (Ed.), Anticancer Drug Development Guide: Preclinical Screening, Clinical Trials and Approval. Humana Press, Totowa, NJ, pp. 101–125; 1997.

18. Holbeck SL, Camalier R, Crowell JA, Govinharajulu JP, Hollingshead M, Anderson LW, Polley E, Rubenstein L, Srivastava A, Wilsker D, Collins JM, Doroshow JH. The national cancer institute ALMANAC: a comprehensive screening resource for the detection of anticancer drug pairs with enhanced therapeutic activity. Cancer Res 2017; 77: 3564–76. [PubMed: 28446463]

19. Monks A, Scudiero D, Skehan P, Shoemaker R, Paull K, Vistica D, Hose C, Langley J, Cronise P, Vaigro-Wolff A, Gray-Goodrich M, Campbell P, Mayo J, Boyd M. Feasibility of a High-flux anticancer drug screen using a diverse panel of cultured tumor cell lines. J Natl Cancer Inst 1991; 83: 757–66. [PubMed: 2041050]

20. Shoemaker RH. The NCI60 human tumour cell line anticancer drug screen. Nat Rev Cancer 2006; 6(10): 813–823. [PubMed: 16990858]

21. Lorenzi PL, Reinhold WC, Varma S, Hutchinson AA, Pommier Y, Chanock SJ, Weinstein J. DNA fingerprinting of the NCI-60 cell line panel. Mol Cancer Ther 2009; 8: 713–24. [PubMed: 19372543]

22. Ritz C, Baty F, Streibig JC, Gerhard D. Dose-Response Analysis Using R. PLoS ONE 2015; 10: e014602.

23. Hollingshead MG, Stockwin LH, Alcoser SY, Newton DL, Orsburn BC, Bonomi CA, Borgel SD, Divelbiss R, Dougherty KM, E Hager EJ, Holbeck SL, Kaur G, Kimmel DJ, Kunkel MW, Millione A, Mullendore ME, Stotler H, Collins J Gene expression profiling of 49 human tumor xenografts from *in vitro* culture through multiple *in vivo* passages - strategies for data mining in support of therapeutic studies. BMC Genomics 2014; 15: 393. [PubMed: 24885658]

24. Pan CX, Zhang H, Tepper CG, Lin TY, Davis RR, Keck J, Ghosh PM, Gill P, Airhart S, Bult C, Gandara DR, Liu E, de Vere White RW. Development and characterization of bladder cancer patient-derived xenografts for molecularly guided targeted therapy. PLoSONE 2015; 10: e0134346.

25. Pratt SE, Durland-Busbice S, Shepard RL, Donoho GP, Starling JJ, Wickremsinhe ER, Perkins EJ, Dantzig AH. Efficacy of low-dose oral metronomic dosing of the prodrug of gemcitabine, LY2334737, in human tumor xenografts. Mol. Cancer. Ther 2013; 12:481. [PubMed: 23371859]

26. (a)Hollingshead M Intraperitoneal and subcutaneous tumor models for assessing anti-neoplastic agents in rodents. Current Protocols in Pharmacology 2002; 5.28.1.(b)Hollingshead M, Alley M, Burger AM, Borgel S, Pacula-Cox C, Fiebig H, Sausville EA In vivo antitumor efficacy of 17-DMAG (17-dimethylaminoethylamino-17-demthoxygeldanamycin hydrochloride), a water-soluble geldanamycin derivative. Cancer Chemother. Pharmacol 2005; 56:115. [PubMed: 15791458] (c) https://dtp.cancer.gov/organization/btb/acute_toxicity.htm.

27. Paul KP, Shoemaker RH, Hodes L, et al. Display and analysis of patterns of differential activity of drugs against human tumor cell lines: Development of the mean graph and COMPARE algorithm. J Natl Cancer Inst. 1989; 81(14):1088–92. [PubMed: 2738938]

28. Holbeck SL, Collins JM, Doroshow JH. Analysis of FDA-approved anti-cancer agents in the NCI60 panel of human tumor cell lines. Mol Cancer Ther 2010; 9(5): 1451–1460. [PubMed: 20442306]
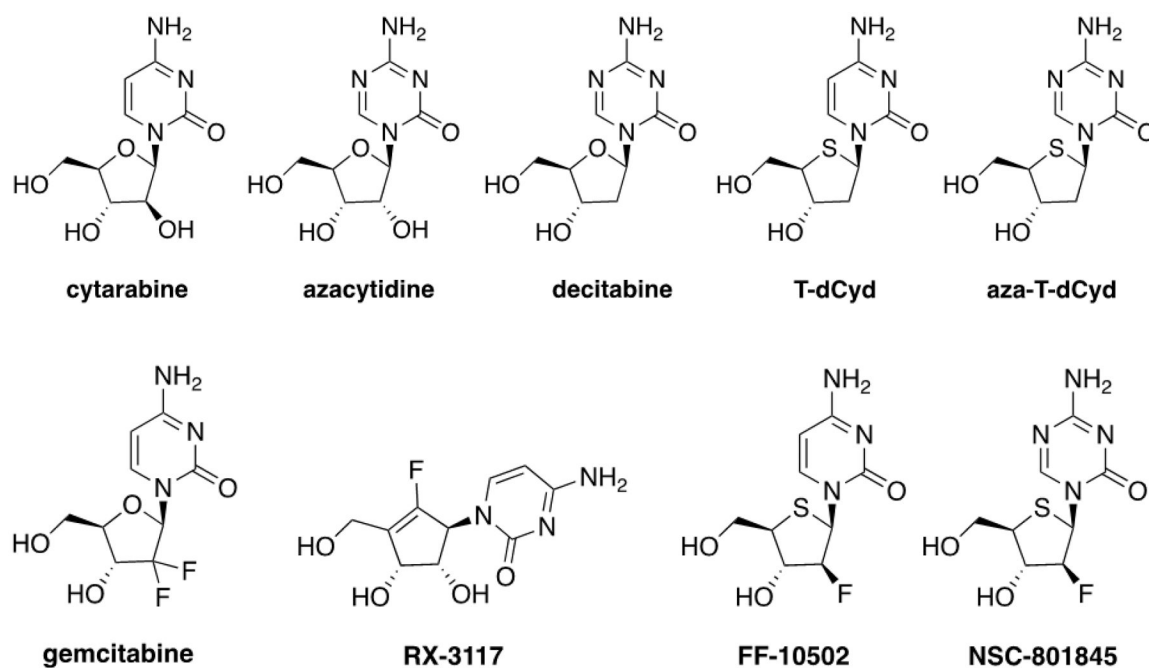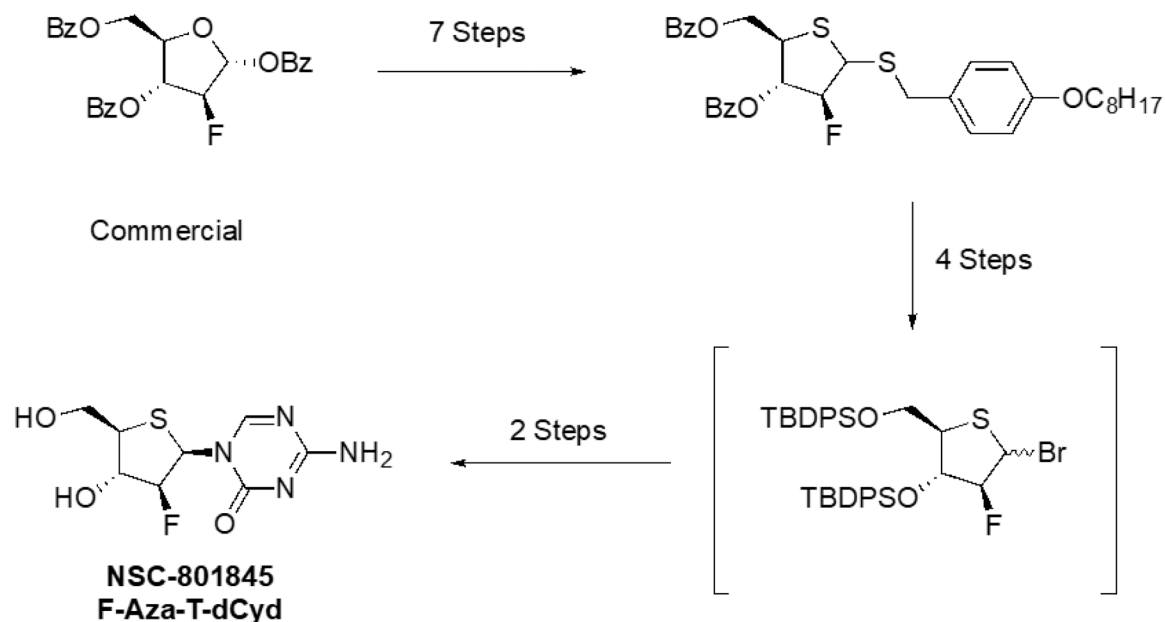
Figure 1.
Chemical structures of cytidine analogs which are FDA-approved drugs, cytatabine, azacytidine, decitabine, and gemcitabine, and investigational agents, 4'-thio-2'-deoxycytidine (T-dCyd), 5-aza-4'-thio-2'-deoxycytidine (aza-T-dCyd), and fluorine containing cytidine compounds, RX-3117 F-T-dCyd (FF-10502) and F-aza-T-dCyd (NSC801845).

Figure 2.
Brief schema for the synthesis of F-aza-T-dCyd (NSC801845). Commercially available
(2*R*,3*S*,4*R*,5*R*)-5-((benzoyloxy)methyl)-3-fluorotetrahydrofuran-2,4-diyl dibenzoate was
used to prepare (4-Octyloxybenzyl) 3,5-di-*O*-benzoyl-2-b-fluoro-2-deoxy-1,4-dithio-D-
erythro-pentofuranoside in seven steps. The brominated 3,5- *t*-butyldiphenylsilyl −2-β-
fluoro-1-thioether was produced in 4 steps. Finally, coupling of the bromide with silylated
aza-cytosine gave the bis silylated 2-β-fluoro-nucleoside in 32% isolated yield which upon
desilylation with tetra-*n*-butylammonium fluoride on silica gel produced 2-β-Fluoro-Aza-T-
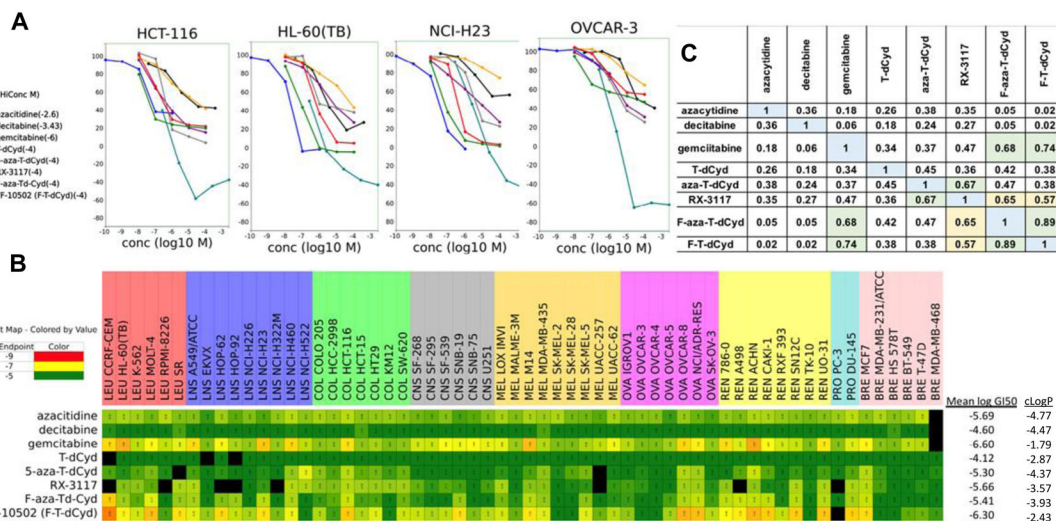dCyd (NSC-801845). The detailed synthetic procedures are in the Supplemental Materials.

Figure 3.

A. Concentration response curves for eight cytidine analogs in four representative human tumor cell lines after 2-days. **B**. NCI-60 screen GI_{50} heat map showing the absolute potency of the eight cytidine analogs across the NCI-60 panel of cell lines. **C**. NCI-60 COMPARE analysis of the eight cytidine analogs based upon the similarity/difference between the NCI-60 response patterns of the compounds where 1 is the compound compared with itself.
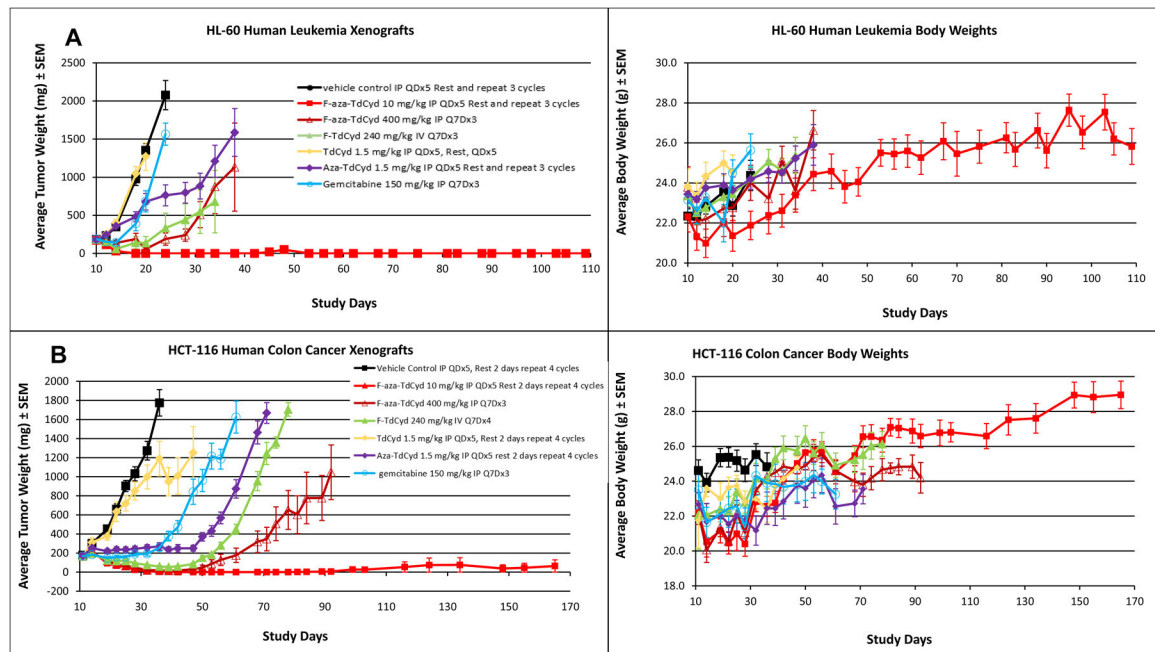
Figure 4.
A. Growth delay of the human HCT116 colon carcinoma grown as a subcutaneous xenograft in female nude mice with each of five cytidine analogs administered in optimized dose and route regimens. Experiments were initiated with groups of 7–8 mice at 6–7 weeks of age and when tumors were 150–200 mm^3 in volume. Data are the mean and standard error for each group (n=16 for vehicle control; n = 8/drug treated group) with data no longer plotted when 50% or less of the animals remained within each group. Mean body weights of groups of mice over the course of the experiment for each treatment group are shown in chart 2. **B**. Growth delay of the human HL-60 leukemia grown as a subcutaneous xenograft in female nude mice with each of five cytidine analogs administered in optimized dose and route regimens. Experiments were initiated with groups of 7–8 mice at 6–7 weeks of age and when tumors were 150–200 mm^3 in volume. Data are the mean and standard error for each group (n=16 for vehicle control; n = 8/drug treated group) with data no longer plotted when 50% or less of the animals remained within each group. Mean body weights of groups of mice over the course of the experiment for each treatment group are shown in chart 2.
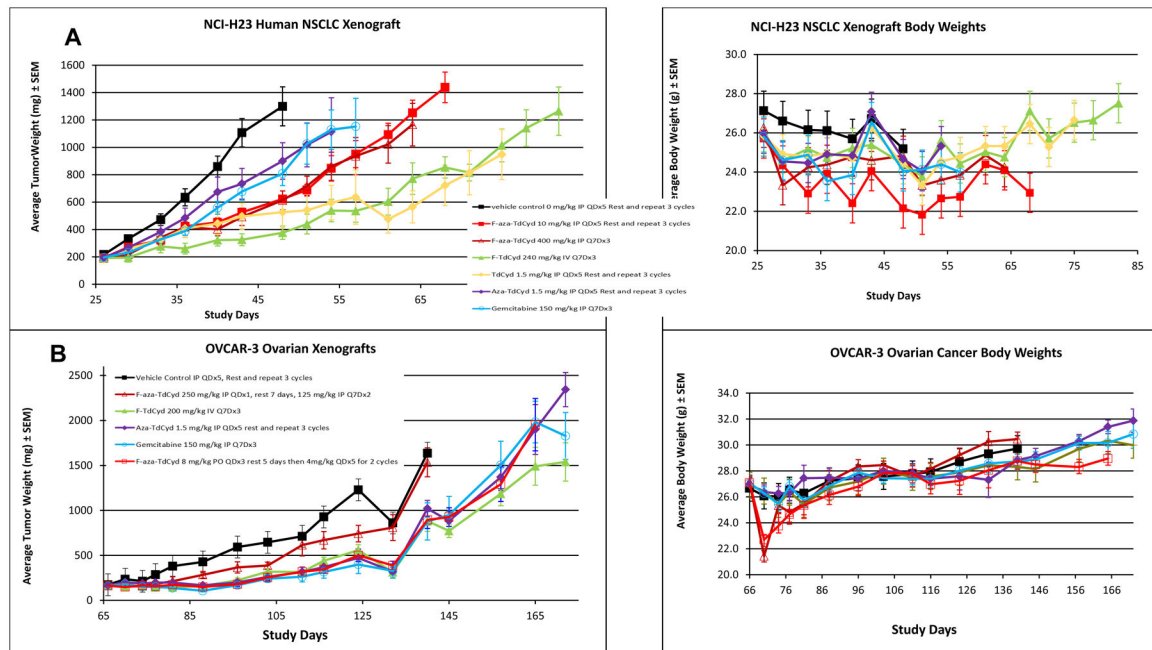
Figure 5.
A. Growth delay of the human OVCAR3 ovarian carcinoma grown as a subcutaneous xenograft in female nude mice with each of five cytidine analogs administered in given dose and route regimens. Experiments were initiated with groups of 7–8 mice at 6–7 weeks of age and when tumors were 150–200 mm^3 in volume. Data are the mean and standard error for each group (n=16 for vehicle control; n = 8/drug treated group) with data no longer plotted when 50% or less of the animals remained within each group. Mean body weights of groups of mice over the course of the experiment for each treatment group are shown in chart 2. **B**. Growth delay of the human NCI-H23 non-small cell lung carcinoma grown as a subcutaneous xenograft in female nude mice with each of five cytidine analogs administered in optimized dose and route regimens. Experiments were initiated with groups of 7–8 mice at 6–7 weeks of age and when tumors were 150–200 mm^3 in volume. Data are the mean and standard error for each group (n=16 for vehicle control; n = 8/drug treated group) with data no longer plotted when 50% or less of the animals remained within each group. Mean body weights of groups of mice over the course of the experiment for each treatment group are shown in chart 2.
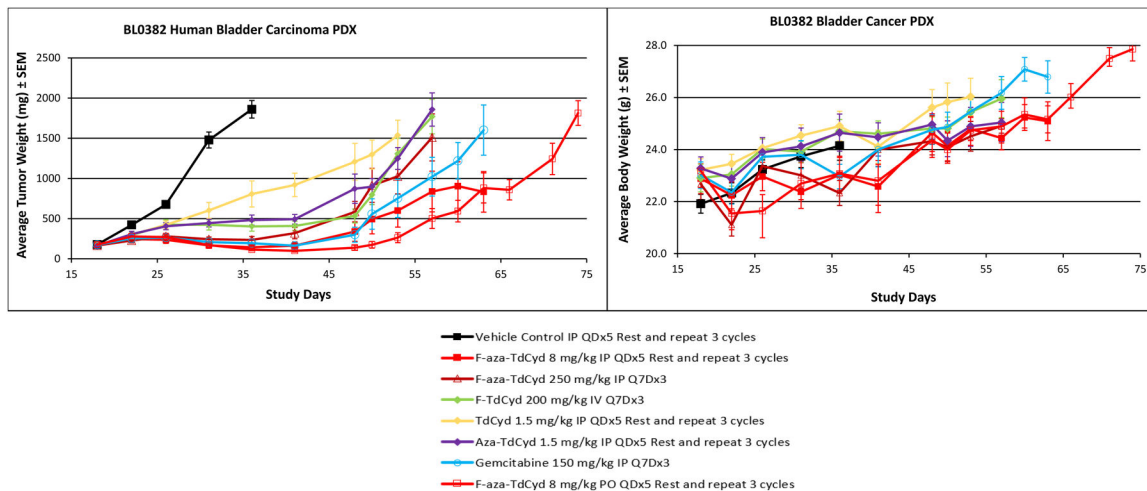
Figure 6.
Growth delay of the patient-derived xenograft, BL0382 bladder carcinoma grown as a subcutaneous xenograft in female NSG mice with each of five cytidine analogs administered in optimized dose and route regimens. Experiments were initiated with groups of 7–8 mice at 6–7 weeks of age and when tumors were 150–200 mm^3 in volume. Data are the mean and standard error for each group (n=16 for vehicle control; n = 8/drug treated group) with data no longer plotted when 50% or less of the animals remained within each group. Mean body weights of groups of mice over the course of the experiment for each treatment group are shown in chart 2.